International Journal of Pharmaceutics 417 (2011) 163–172

Contents lists available at ScienceDirect

International Journal of Pharmaceutics

journal homepage: www.elsevier.com/locate/ijpharm

Pharmaceutical applications of non-linear imaging

Clare J. Strachan [a,*], Maike Windbergs [b], Herman L. Offerhaus [c]

[a] School of Pharmacy, University of Otago, P.O. Box 56, Dunedin 9054, New Zealand
[b] School of Engineering and Applied Sciences, Harvard University, 58 Oxford Street, Cambridge, MA 02138, USA
[c] Optical Sciences Group, MESA+ Institute for Nanotechnology, University of Twente, Postbus 217, 7500 AE Enschede, The Netherlands

ARTICLE INFO

Article history:
Received 17 October 2010
Received in revised form
14 December 2010
Accepted 15 December 2010
Available online 21 December 2010

Keywords:
Non-linear imaging
Coherent anti-Stokes Raman scattering (CARS) microscopy
Second harmonic generation
Two-photon fluorescence
Dosage form
Drug delivery

ABSTRACT

Non-linear optics encompasses a range of optical phenomena, including two- and three-photon fluorescence, second harmonic generation (SHG), sum frequency generation (SFG), difference frequency generation (DFG), third harmonic generation (THG), coherent anti-Stokes Raman scattering (CARS), and stimulated Raman scattering (SRS). The combined advantages of using these phenomena for imaging complex pharmaceutical systems include chemical and structural specificities, high optical spatial and temporal resolutions, no requirement for labels, and the ability to image in an aqueous environment. These features make such imaging well suited for a wide range of pharmaceutical and biopharmaceutical investigations, including material and dosage form characterisation, dosage form digestion and drug release, and drug and nanoparticle distribution in tissues and within live cells. In this review, non-linear optical phenomena used in imaging will be introduced, together with their advantages and disadvantages in the pharmaceutical context. Research on pharmaceutical and biopharmaceutical applications is discussed, and potential future applications of the technology are considered.

1. Introduction

Linear (absorption), phase contrast and fluorescence microscopies have all proven extremely useful over the years and much can be achieved by them but they cannot fulfil all requirements. The key advantages of non-linear techniques over linear techniques are: (1) better selectivity in the excitation, which leads to label-free imaging and optical sectioning; and (2) better selectivity in the output, which creates possibilities for more sensitive detection. These advantages stem from the non-linear nature of the interaction with the sample. In general, a non-linear optical process involves two or more photons going into the sample and interacting in a manner that creates a photon of some other wavelength which is then detected (Boyd, 2008).

Since the non-linear process requires several photons (or light fields) it depends (linearly) on the intensity of each of these photons (fields) and therefore non-linearly on the overall intensity. This non-linear dependence means that focused beams will generate a signal predominantly in the focal region, making the process inherently confocal (Fig. 1). Furthermore, the interaction of multiple photons implies a number of ways in which the photons can combine to find a resonant enhancement. In the case of resonances at the frequency difference between two incoming (optical) photons, the difference is somewhere in the near-infrared to infrared, where very specific resonances can be found for molecular bonds between molecules and groups of molecules. Linear absorption targets the electronic transitions which are less specific for molecular structure.

Even if the photons are all present at the right time, they also need to combine with the right phase to generate an overall signal that can be detected. This is generally constrained by the so-called phase-matching conditions (conservation of momentum) and selection rules. These restrictions are not all bad; they suppress second harmonic generation (SHG) for all materials with inversion symmetry, but that means that SHG can be used for selective analysis of boundary layers where the inversion is locally broken. They tend to restrict the emission in bulk to the forward direction, which means that small inclusions have a relatively enhanced emission in the backward direction. If the photons have been combined to form a new photon, this photon comes out with a well defined frequency (and phase). This predictable (new) frequency allows for spectrally separated detection that can sometimes avoid problems such as auto-fluorescence.

For application in pharmaceutical research three advantages are especially important: label-free (chemically selective) detection, spatial selectivity and (for dynamic processes) imaging speed. Labels are best avoided because they alter the structure and, to a greater or lesser degree, the physicochemical or biological proper-

* Corresponding author. Tel.: +64 3 479 7324; fax: +64 3 479 7034.
E-mail addresses: clare.j.strachan@otago.ac.nz (C.J. Strachan), windb@seas.harvard.edu (M. Windbergs), h.l.offerhaus@utwente.nl (H.L. Offerhaus).

0378-5173/$ – see front matter © 2010 Elsevier B.V. All rights reserved.
doi:10.1016/j.ijpharm.2010.12.017

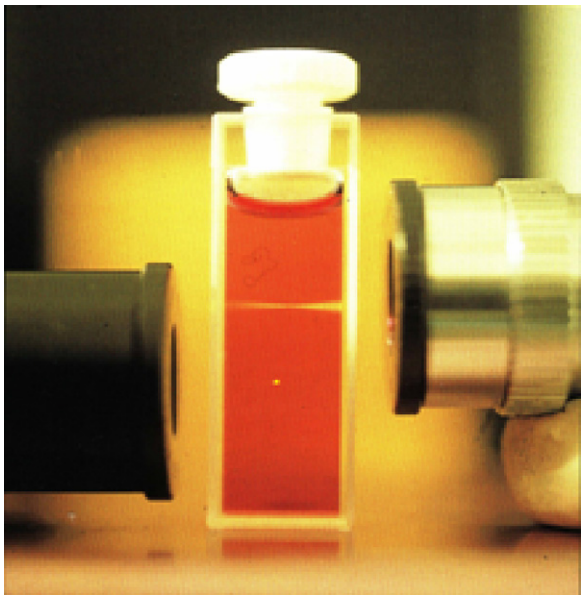

Fig. 1. The top shows one-photon fluorescence from right and the bottom shows two-photon fluorescence from the left.
Image by Brad Amos, MRC, Cambridge.

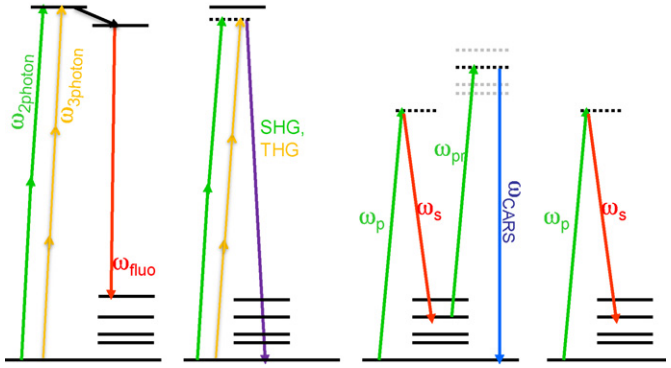

Fig. 2. Energy level diagrams of the different non-linear optical events. The first diagram on the left shows two- and three-photon fluorescence where either two or three photons reach a real (solid line) electronic state. After some internal conversion a fluorescent photon is emitted. The second diagram shows second- and third-harmonic generation where a virtual state (dashed line) is accessed. This level can be close to a resonant level. The third image shows the CARS process where a pump and Stokes photon combine to reach a real vibrational level. Probing of this level results in the CARS photon. The final diagram shows Raman scattering. In spontaneous Raman scattering the Stokes photon is emitted and detected on a spectrometer. In SRS both pump and Stokes fields are supplied externally and the effect of one field on the other is measured.

ties of the molecule of interest (Carvell et al., 1998). The selectivity is required to analyse the composition, and the spatial resolution allows the composition to be analysed locally, which ideally should be below the size of the components of interest. Furthermore, the imaging speed is necessary for real time monitoring of processes such as drug release from dosage forms and drug interactions with tissues and cells.

Biomedical applications of imaging using non-linear optics is a comparatively well established field, with several reviews covering various aspects of the area (Evans and Xie, 2008; Oheim et al., 2006; Tsung-Hua et al., 2009). Pharmaceutical applications of non-linear imaging are much less widely explored. However, since the advantages of non-linear optics are similar with respect to both types of application, it is expected that research into pharmaceutical applications of non-linear imaging will grow rapidly.

We will introduce a number of non-linear techniques that are currently used in pharmaceutics and discuss their particular strengths and weaknesses. We neglect non-linear processes based on pump–probe interactions and strong-field coherent control in this discussion because they are especially suited for studying fast temporal dynamics, which is less relevant here. Raman microscopy using spontaneous Raman scattering is covered in another article in this special issue (Gordon and McGoverin, this issue). The applications covered in this review span both pharmaceutical and biopharmaceutical contexts. Firstly, the characterisation of drugs and different types of dosage forms is discussed, followed by the analysis of dosage form changes during drug release. Imaging the fate of drugs (and nanoparticles) in tissues and within cells is then considered. Potential future applications are also discussed.

2. Non-linear imaging techniques

Non-linear imaging (also called multi-photon imaging) techniques can be classified along two directions, the number of photons involved and the level of coherence of the output. Incoherent techniques are two- and three-photon fluorescence. These provide selectivity (contrast) on the resonances in the (mostly) electronic absorptions, and sometimes there is additional selective information in the output (fluorescence) spectrum and the fluorescence lifetime. Spontaneous Raman imaging also falls into this category but it does not depend on the existence of a fluorescent state, and provides very high (label-free) selectivity and has a low cross-section. The combination of these properties makes it more like the coherent techniques in practice. The coherent techniques are second harmonic generation (SHG), sum frequency generation (SFG), difference frequency generation (DFG), third harmonic generation (THG), coherent anti-Stokes Raman scattering (CARS), stimulated Raman scattering (SRS) and variations thereof. Energy level diagrams of the different non-linear optical events are shown in Fig. 2.

2.1. Two- and three-photon fluorescence

For two- and three-photon fluorescence, the main advantage of the non-linearity is in the spatial selectivity due to the non-linear excitation. Chemically selective excitation comes from the electronic resonances in the absorption and from differences in the emission of different materials. In general one has to move more to the near-infrared for the excitation wavelength in three-photon excitation to retain specificity on the absorption. The long excitation wavelength can have significant advantages in avoiding damage through linear absorption and heating. The spatial resolution is generally around a few hundred nanometers. The sources and setup are relatively simple, with a single femto- or pico-second excitation source and a photomultiplier tube for the detection. Since the cross-sections tend to be quite high, the collection of sufficient signal is relatively easy and imaging speeds can be high (<1 s per image).

Spontaneous Raman imaging, or hyperspectral Raman imaging, employs a single input wavelength that can be tuned close to an electronic resonance, and collects a spectrum of the inelastically scattered photons. The input wavelength has to be blocked carefully (the amount of scattered light is very low and any residual input would swamp the signal) and fluorescence has to be avoided by a careful choice of input wavelength. The collection of the spectrum requires many photons so that Raman imaging tends to be somewhat slow (tens of minutes per image). However, once the spectrum has been collected it can be used to unravel the composition of the sample to a high degree of accuracy (see Gordon and McGoverin, this issue).

2.2. Coherent mixing processes

Non-resonant second harmonic generation (SHG) was first demonstrated by Franken and co-workers in 1961 (McFearin et al., 2009), shortly after the invention of the laser. It was soon realised that in any system with inversion symmetry no second harmonic is generated. However in structures that break the symmetry, such as chiral structures or on boundaries between materials, second harmonic can be generated. This generation is a parametric process, which is to say that the emission is phase-coherent with the excitation. This phase-coherence causes the output to be a coherent beam of light rather than random emission in all directions. This makes it much easier to collect the signal on a detector and makes it possible to detect generated signals by beating them against an (externally generated) source and to obtain detection with high sensitivity. Typical structures that can be seen by SHG are starch and collagen, or fibrillic and laminar structures.

Sum frequency generation (SFG) is a more general case of second harmonic generation, where two different input lasers are used to create the sum-frequency of the two. Although two input lasers require a more complicated setup than just one, it opens up the possibility of resonant enhancement by using one frequency that is resonant with some transition. Surface spectroscopy of self assembled monolayers or boundary layers has been achieved with very good sensitivity using an infra-red (IR) photon and a visible photon (see for example, McFearin et al., 2009). The IR photon ensures the selectivity by its resonance with some transition, and the mixing with the visible photon ensures the selectivity to the boundary layer and a reasonable resolution.

What can be done with two photons can also be done with three. One advantage of third harmonic generation (THG) over SHG is that the requirement for the lack of inversion symmetry is lifted. Most materials will have some third harmonic response and, even if the material as a whole lacks inversion symmetry, a signal can be obtained. There is, however, still the requirement of phase matching, which tends to cancel signals in homogeneous materials for focused beams (as one would use in a microscope). This cancellation stems from the Gouy shift that all light encounters when going through a focus (see for example, the treatment by Boyd, 2008). In THG, the wavelength of the third harmonic is so different from that of the fundamental that the generated light shifts differently to the fundamental. As a result, light generated before the focus destructively interferes with the light that is generated after the focus. This makes THG (like SFG) sensitive for transitions and surfaces, and sensitive for the detection of blood vessels and other biological structures (Carriles et al., 2009).

CARS, like THG, depends on the third order non-linearity but employs a resonance at the difference frequency between two of the input frequencies to enhance the signal. The shorter frequency is generally called the pump and the lower frequency the Stokes. When the frequency difference between them matches a vibrational resonance in the sample, the polarisation is enhanced. When the third photon (the probe photon, which is often another pump photon) probes the polarisation, a signal is generated at a frequency higher than the pump, and this is called the anti-Stokes or CARS signal. CARS requires phase matching so that different frequencies must be at angles with respect to one another. In microscopy this requirement is circumvented by using microscope objectives with such a high numerical aperture that the required k-vectors are always present and the interaction volume is too short for dephasing.

Given the low yield of high-order non-linear processes, some effort has been put into optimising performance. To optimise the interaction with a single vibrational level, the pulse duration of the incoming light has to be as short as possible, as long as the bandwidth fits within the bandwidth of the transition. In general this means pulses of a few picoseconds duration. Due to the coherent excitation and emission of all the molecules in the focal volume, the amplitudes add coherently and the output scales quadratically with the number (density) of molecules. This is nice for the majority species but can limit the detection of minority species. Similarly, a non-resonant majority can generate a very large non-resonant background that interferes with the resonant signal and can overwhelm a small signal. This non-resonant background exists even in pure substances because multiple pathways exist to the CARS wavelength. Many approaches have been developed to reduce this background, such as polarisation control (Oudar et al., 1979; Yuratich and Hanna, 1977), time-delay (Volkmer et al., 2002; von Vacano and Motzkus, 2006), frequency modulation (Ganikhanov et al., 2006) and interferometric detection (Cheng, 2007; Evans et al., 2004; Müller and Zumbusch, 2007). The last has the advantage that the amplitude and phase are detected, where the amplitude is linear in the number (density) of the molecules. If the phase is extracted in a clean method it can also be used to detect multiple molecules simultaneously (Jurna et al., 2010). The narrowband (single vibrational transition) CARS has been very successful for the imaging of species with a reasonably high concentration or strong transition dipoles, such as many types of lipids (C–H vibration), phenols and phosphates (Cheng, 2007; Cheng and Xie, 2004; Müller and Zumbusch, 2007). Image collection rates can be quite fast (< 1 s per image).

When detection of a single transition does not yield sufficient specificity, a broadband technique can be employed that reveals multiple transitions at once. This requires pulses with a much wider bandwidth. Often the bandwidth from the laser sources is enhanced by soliton formation (Groß et al., 2010) or continuum generation. Generally the Stokes (and/or pump) band is broadened while the probe is kept narrow so that the vibrational signatures are in the CARS output as narrow spectral features. Since a spectrum must be collected point-by-point, which requires many more photons, the imaging speed is reduced. The broad bandwidth also tends to induce more non-resonant background. This background can, however, be used as a type of local oscillator, and with some assumption (Liu et al., 2009; Rinia et al., 2007), the background can be used to extract amplitude and phase information. More complex arrangements can be made when the phase of the broadband light is controlled (Oron et al., 2002; van Rhijn et al., 2010).

Stimulated Raman scattering (SRS), stimulated absorption and stimulated emission do not produce a new wavelength, which makes them fundamentally different from the other coherent parametric processes. SRS employs the same pump and Stokes input as CARS but does not use another photon to produce a CARS photon, so a lower intensity can be used. Since the cross-section for Raman scattering is very low, the absorption due to the Raman scattering cannot be measured directly. However, by stimulating this transition and modulating the stimulation by some high frequency, where the amplitude fluctuations of the laser sources are very low (above 1 MHz), it is possible to measure the small (10^{-6}) variation of the pump transmission that is induced by the presence of the Stokes (Freudiger et al., 2008). There is no non-resonant background in SRS since it measures the disappearance of photons at the Stokes frequency and there is only one direct resonant channel for this loss. There are other possible interactions that might cause similar loss such as stimulated absorption, stimulated emission and cross-phase modulation but these can be avoided by a careful choice of wavelength and modulation scheme. Imaging speed can be at least as high as CARS (< 1 s per image). Using a broadband Stokes or pump, the Raman loss (or gain) can be measured spectrally. Collection of a full spectrum per pixel is more time-consuming (minutes per image) (Mallick et al., 2008; Ploetz et al., 2009), but makes it possible to distinguish more components. Using a controlled spec-

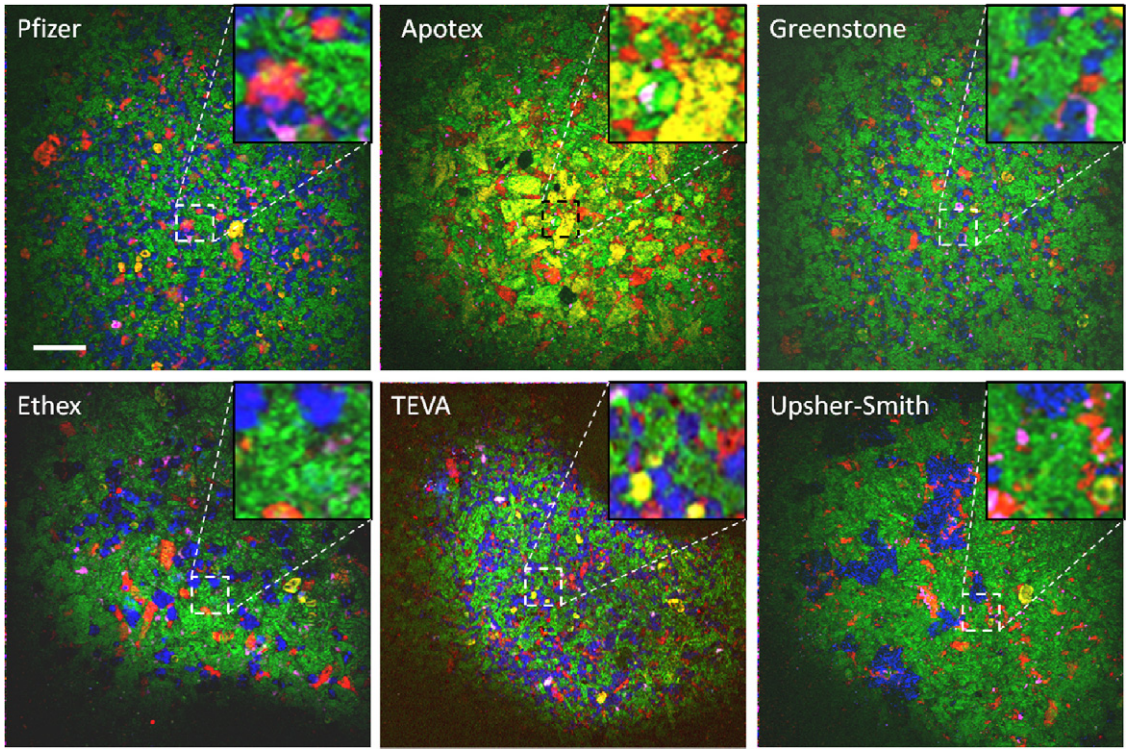

Fig. 3. Tablets from different suppliers imaged with SRS microscopy. Green and blue represent microcrystalline cellulose and dibasic calcium phosphate anhydrous, red indicates the drug amlodipine besylate and magenta represents magnesium stearate. Yellow indicates sodium starch glycolate, with the exception of the tablet provided by Apotex where yellow corresponds to corn starch and lactose monohydrate. The inserts represent four-fold magnifications of the images highlighted with dashed lines. The scale bar denotes 200 μm. (For interpretation of the references to colour in this figure legend, the reader is referred to the web version of the article.)
Reproduced by the permission of the Royal Society of Chemistry (Slipchenko et al., 2010).

tral content, some broadband (multi-line) information can also be extracted from the integrated signal at high imaging speed.

Since many of these techniques require high intensity input pulses it is common for a number of non-linear processes to occur simultaneously. Since they have different advantages, resonances and specificities it is advantageous to collect a combination of these signals at the same time. This is what is often referred to as "multi-modal" imaging. In general CARS, SRS or Raman will be used for high specificity and SHG/THG or auto-fluorescence will be used to determine more structural information (Cheng, 2007).

3. Applications

3.1. Pharmaceutical materials and drug delivery systems

Infrared, near-infrared and spontaneous Raman scattering imaging have been widely used for the analysis of drugs, excipients and dosage forms for over a decade (Clark et al., 2007; Gendrin et al., 2008; Gordon and McGoverin, this issue). The higher spatial and temporal resolutions of the non-linear imaging methods covered in this review lend them to the analysis of a wide variety of systems – both liquid and solid. Chemically selective visualisation of component distribution in complex mixed systems is possible up to a resolution of approximately 200 nm. Physical forms (e.g. solid state form and emulsion droplets) can also be imaged, and dynamic processes, such as crystallisation and emulsion droplet formation, can be followed in real time.

For solid materials and dosage forms, analysis is largely restricted to the sample surface, which may be imaged in three dimensions. Slipchenko et al. (2010) used SRS microscopy to investigate the chemical component distribution in six tablets provided by different manufacturers. Each tablet contained the drug amlodipine besylate and four excipients. Each component could be chemically resolved with the exception of lactose monohydrate and corn starch, which had similar Raman scattering intensities in the spectral region of interest (Fig. 3). The spatial distribution patterns of the drug particles were similar for the different suppliers, but the amount, particle size and distribution pattern of the excipients were unique for each formulation. In the same study, SRS microscopy was compared to CARS and confocal Raman (point-by-point mapping) microscopy in terms of speed, chemical selectivity and spatial resolution. Under the predefined measurement conditions SRS microscopy was much faster than confocal Raman mapping and showed a slightly superior chemical selectivity compared to CARS microscopy, due to a lack of non-resonant background signal (which was present with the CARS analysis). This study demonstrates the potential of non-linear imaging methods (and specifically SRS in this case) for high speed screening of drug and excipient distribution in solid dosage forms, which can be used for analysis during development as well as end-product control. The level of detail obtained is greater than with either pharmacopeial wet chemistry methods or non-destructive spectroscopic analysis approaches with probes (e.g. NIR and Raman) during, for example, content uniformity testing.

CARS microscopy has also been used to image the effect of processing conditions on drug distribution in matrices. Extrusion of the drug theophylline with the solid lipid tripalmitin led to lower surface exposure of the drug compared to that for matrices prepared by direct compression (Jurna et al., 2009; Windbergs et al., 2009). In future, different solid state forms, in addition to chemical components, could be imaged, leading to improved understanding of solid state transformations during processing and storage.

Non-linear imaging techniques can also be applied in the early stage of pharmaceutical development to investigate the phase behaviour in liquid and semi-solid dosage forms. In the case of emulsion based systems, droplet formation dynamics are often

unclear, and clarification about the underlying mechanisms and factors influencing droplet formation are valuable during the development of new dosage forms. In this context, Pautot et al. (2003) investigated the spontaneous formation of emulsion droplets and multilamellar structures called onions. The system under investigation consisted of water and dodecane containing phospholipids. In addition to characterisation on the bulk level using surface tension and light scattering, phenomena at the interface of the two liquids were imaged using CARS microscopy. During this study the origin of spontaneous emulsification was elucidated as the formation of a hydrated semicrystalline multilamellar film at the interface. CARS microscopy was used to identify the onion structure components. The shell was found to consist of partially hydrated concentric bilayers. Moreover, temperature affected the composition and this phenomenon could be correlated to changes in hydration of the lipid bilayer at the interface of water and dodecane. In addition, the concentration of the lipid was found to affect the organisation of the structures.

Dynamic three-dimensional structures associated with surfactants were investigated by Kennedy et al. (2005). Myelin figures, a specific dynamic instability, occurring in a surfactant lamellar phase during swelling and dissolution were analysed. The polarisation sensitivity of CARS microscopy along with its speed was successfully used to image the molecular composition and orientation of the different components inside myelin figures in systems containing water and various surfactants. As the growth rate of such structures is around 2 $\mu m\, s^{-1}$, CARS microscopy was capable of *in situ* analysis of these structures. It was previously believed that myelin structures consisted of tubular structures bearing multiple surfactant bilayers which are concentrically wrapped around a water core structure. The CARS analysis revealed that there is, in fact, no water core, and the myelin figures are instead composed of concentric bilayers with partially ordered water layers between adjacent bilayers. The packing structure inside the myelin figure was found to be highly dependent on the properties of the surfactant.

Chowdary et al. (2010) used non-linear interferometric vibrational spectroscopy to analyse six different commercially available vegetable oils with a focus on the degree of unsaturation in the chemical structures in the samples. It was possible to identify unsaturated structures and detect their relative degrees of unsaturation.

In conclusion, non-linear imaging techniques provide versatile possibilities to investigate the chemical and physical composition of solid and liquid samples, as well as dynamic processes in different systems. Based on these studies, a deeper understanding of both chemical and physical structures and their changes in dosage forms can be achieved, which aids in the rational design of new pharmaceutical formulations.

3.2. Drug release and digestion

The release of the drug from a dosage form is a critical quality attribute since the therapeutic efficacy depends on this very characteristic. In general, drug release is investigated by performing standardised dissolution testing, which involves analysing the concentration of the dissolved drug in a predefined volume of circulating dissolution medium over time. Since the release of the drug is affected by a combination of different factors including the structural characteristics of the dosage form and associated changes during drug release, concentration profiles alone often do not provide enough information to completely understand the drug release. More insight can be achieved with the simultaneous chemically (and physically) selective *in situ* imaging of the dosage form. Non-linear imaging techniques provide promising analytical opportunities to bridge this gap.

Tablets and extrudates have been imaged as representatives of oral solid dosage forms, with CARS microscopy used to better understand drug release (Jurna et al., 2009; Windbergs et al., 2009). A purpose-built flow-through cell was used to provide pharmaceutically relevant dissolution testing conditions and allow the simultaneous analysis of the dosage form using CARS microscopy and solution using UV–vis absorption. A predefined volume of dissolution medium was circulated through the cell while CARS microscopy was used to image the solid dosage form changes. The release of theophylline from the matrix could be visualised in real time, as well as the transformation of the drug particles from the anhydrate to the less soluble monohydrate form, and subsequent dissolution of the monohydrate (Fig. 4). In future, non-linear optical imaging could be used for real-time imaging of many kinds of oral solid dosage forms during dissolution testing, in order to better understand drug release profiles. Obvious candidates for such analysis are sustained release dosage forms and formulations containing metastable and unstable forms of Biopharmaceutical Classification System Class II drugs.

Kang et al. (2006) investigated the three-dimensional distribution of the drug paclitaxel in different polymer films with CARS microscopy. The films served as equivalents for stent coatings used in percutaneous coronary revascularisation. The films were immersed into water to image the release of the drug from the system (Kang et al., 2006). The authors also studied component distribution and drug release from spray-coated films consisting of polyethylene glycol (PEG)/poly (lactide-co-glycolic-acid) (PLGA) blends (Kang et al., 2007). The drug and polymers were individually imaged with CARS microscopy. For those films consisting of pure polymer blends without any drug loading, phase segregation was detected. For blends containing 10–40 wt% PEG, the PEG phase formed crystalline fibers in the percolating PLGA matrix. In drug loaded formulations the drug was preferentially located in PEG domains. The PEG and drug formed a solid dispersion, with the absence of PEG crystals being confirmed using X-ray powder diffraction. Furthermore, the release of the drug was analysed as the film was exposed to an aqueous solution. CARS microscopy could successfully be used to image the distribution and monitor reorganisation of PEG and the drug during the release process.

Of particular relevance to lipid-based drug delivery systems such as emulsions, microemulsions, and self-microemulsifying systems (SMEDDS), multiplex CARS imaging of lipid digestion and its interaction with lipophilic drug disposition has recently been performed (Day et al., 2010). First, the researchers imaged the digestion of pure lipid droplets, specifically glyceryl trioleate, in an emulsion containing porcine pancreatic lipase. The undigested oil and lipolytic products were resolved, with lipolysis occurring at the oil–aqueous phase interface, consistent with the enzyme being present in the aqueous phase. In addition, since the CARS spectra also depended on the phase of the components imaged, crystallisation of the lipolytic products could also be observed (Fig. 5). Of particular interest, the authors also studied the fate of lipophilic drugs present in the lipid drops during the digestion process. Ergosterol, present as a crystalline suspension in the lipid droplets, dissolved in the mixed micelles forming after lipolysis, a step necessary for the uptake of sterols into the body. The lack of crystallisation of the lipolytic products suggests that the sterol itself also affected the lipolytic product phase behaviour. The concentration of two lipophilic drugs, vitamin D and progesterone, was quantitatively mapped within emulsion droplets as a function of the digestion process. The spectral signatures allowed concentrations down to about 5 and 20 mM for the two drugs respectively. In the absence of enzyme, the droplet sizes remained constant, but the drug concentration decreased due to solubilisation in bile salt micelles present in the buffer solution. However, in the pres-

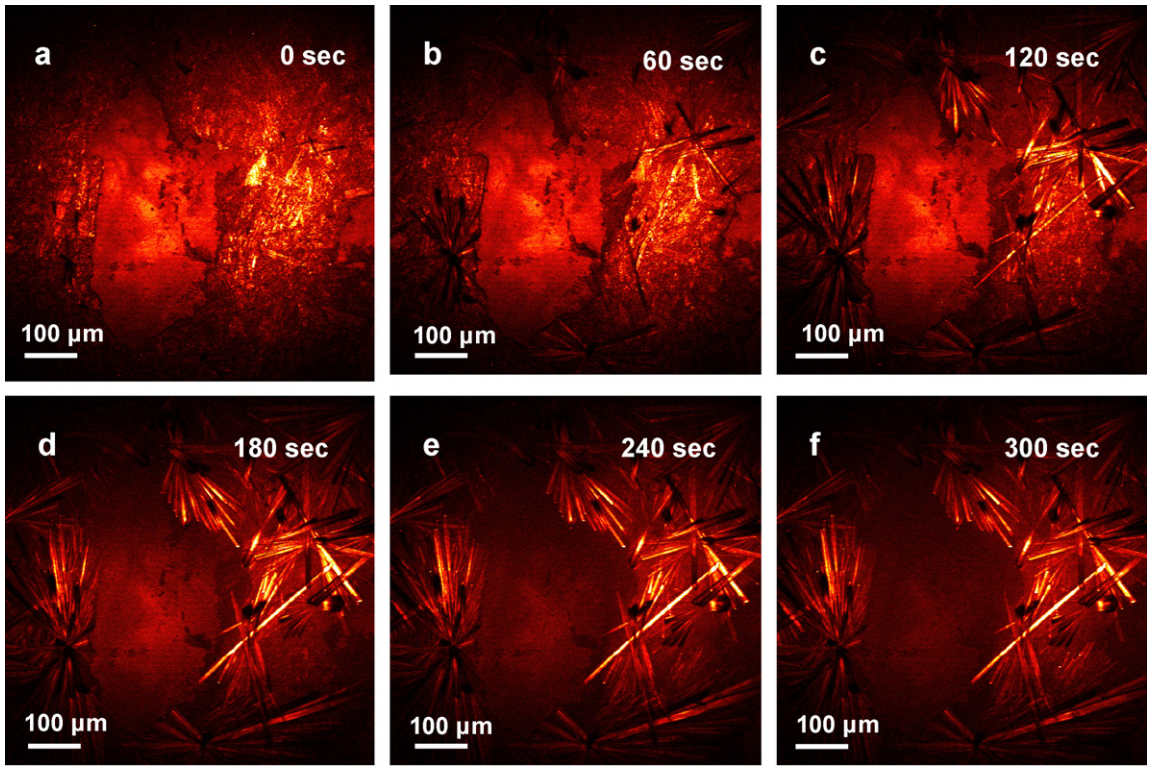

Fig. 4. *In situ* visualisation of crystal growth on a tablet surface in dissolution medium. Originally, the tablet consisted of theophylline anhydrate embedded in a lipid matrix. The drug recrystallises in the less soluble monohydrate form. Reproduced by permission of the American Chemical Society (Windbergs et al., 2009). Video can be accessed at http://pubs.acs.org/doi/suppl/10.1021/ac8020856.

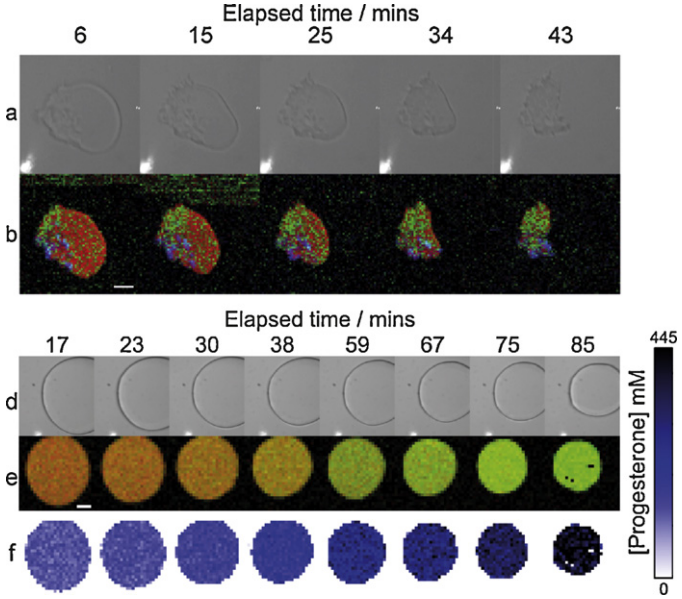

Fig. 5. Time resolved images of the digestion lipid droplets by porcine pancreatic lipase. The top image shows a glyceryl trioleate droplet containing ergosterol ((a) light microscopy image and (b) CARS false colour image with glyceryl trioleate in red, lipolytic product in green, and ergosterol in blue, scale bar = 5 μm). The bottom image shows a glyceryl trioctanoate droplet containing progesterone, at an initial concentration of 95 mM ((d) light microscopy image, (e) CARS false colour image with glyceryl trioctanoate in red and progesterone in green, (f) false colour images of the concentration of progesterone within the droplet (concentration given by colour bar, the scale bar denotes 10 μm). (For interpretation of the references to colour in this figure legend, the reader is referred to the web version of the article.) Reproduced by the permission of the American Chemical Society (Day et al., 2010).

ence of enzyme, the drugs concentrated as the lipid droplets were hydrolysed, presumably due to the low solubility of the drugs in the lipolysis products (Fig. 5). Although this suggests that glyceryl trioleate may not be the most appropriate drug delivery medium for these drugs, the study demonstrates the value of such analysis for identifying lipid-based drug delivery systems that efficiently release the drug from the oily phase during lipid digestion.

These examples demonstrate that non-linear imaging techniques are well suited to the analysis of drug release from different drug delivery systems. Real time visualisation of processes affecting drug release, such as recrystallisation of less soluble solid state forms of the drug or reorganisation of components, as well as interactions, can be monitored. Furthermore, the fate of dosage forms in the body could be mimicked in terms of interactions with physiological fluids. Non-linear imaging techniques allow a broad range of *in situ* analyses of drug release and interactions with body fluids/digestion, which have not been accessible with other techniques.

3.3. Imaging drugs in tissues and cells

The fate of drugs and nanoparticles in tissues and cells has been most commonly investigated using confocal microscopy, either together with dyes or by tagging the molecules or nanoparticles with fluorescent probes. In the last two decades, non-linear fluorescent imaging has been increasingly used to improve spatial resolution, reduce photolytic damage to the cells, and increase the possible sampling depth within tissues. Some autofluorescing drugs can be imaged without modification using two-photon fluorescence. For non-autofluorescing materials, other non-linear optical methods can be employed if the analytical sensitivity is sufficient.

3.3.1. Dermal and transdermal drug delivery

The imaging of dermal and transdermal drug delivery using non-linear optics has been researched for almost a decade. The use of two-photon fluorescence and SHG for these and other dermatological applications has been reviewed (Lin et al., 2007; Tsung-Hua et al., 2009). Collagen and some other non-centrosymmetric structures have been imaged using SHG, while two-photon fluorescence has been used to probe autofluorescing pharmaceutical compounds and keratin. More recently, CARS microscopy and SRS have been used to image lipids and non-fluorescing compounds of pharmaceutical interest.

The first studies involved the imaging of autofluorescing model molecules intended to mimic drugs in the presence of oleic acid, a penetration enhancer (Yu et al., 2001, 2003). The three dimensional spatial distributions of the hydrophilic sulphorhodamine B and hydrophobic rhodamine B hexyl ester were imaged using two-photon fluorescence and were found to be distributed both within the corneocytes and, at a higher concentration, in the intercellular lipidic regions in the stratum corneum. The analysis suggests that both drugs penetrated the skin via both inter- and intracellular pathways in the absence of oleic acid. However, although the penetration of both drugs was enhanced by oleic acid, the oleic acid led to increased partitioning of the hydrophobic drug into the more lipophilic intercorneocyte regions, while the hydrophilic drug concentrated within the corneocytes. Lee et al. (2008) have studied the influence of the depilatory agent thioglycolate on the penetration of the same molecules, and, by simultaneously imaging the autofluorescing intracellular keratin, they could observe the homogenisation of the corneocyte structure and cellular detachment in the presence of the penetration enhancer, which can be associated with increased drug penetration through the stratum corneum (Lee et al., 2008). Increased disorder in the intercellular lipid lamellae in the presence of oleic acid has also been established (Sun et al., 2004).

Near-infrared light commonly used for non-linear imaging can penetrate past the stratum corneum and into the dermal layer. Recently, Freudiger et al. (2008) used SRS to investigate the epidermal and dermal penetration of dimethyl sulphoxide (DMSO), a penetration enhancer, and retinoic acid, used to treat acne and reduce wrinkles and photoaging. Bands at 670 cm^{-1} and 1570 cm^{-1} were used to image DMSO and retinoic acid respectively, while endogenous lipids in the skin were imaged using the CH_2 stretching mode at 2845 cm^{-1} (Fig. 6). The authors were able to probe up to about 90 μm into intact murine ear skin tissue, and found that DMSO penetrated up to about 65 μm into the skin after administration of 20/80 (v/v) water/DMSO to the skin surface for 1 h at 37 °C. The relatively hydrophilic DMSO partitioned into the protein/aqueous rich regions. The bulkier retinoic acid molecules were imaged only about 20 μm into the skin after administration of retinoic acid. The more lipophilic molecules appeared to penetrate primarily via the intercellular lipid-rich phase in the epidermis. CARS microscopy has also been used to image drug penetration. Administered retinol has been found to congregate in the interstitial space between the corneocytes of the stratum corneum in murine ear skin (Evans and Xie, 2008), and mineral oil was also found to penetrate the stratum corneum of the mouse ear via the same pathway, with the oil being restricted to the epidermal layer (Evans et al., 2005). The penetration of nanoparticles into skin has also been investigated (Kuo et al., 2009; Mortensen et al., 2008; Stracke et al., 2006) and, using SHG, penetration enhancers were found to facilitate the penetration of zinc oxide particles (Kuo et al., 2009).

These studies demonstrate that non-linear imaging can provide insight into the localisation of drugs and nanoparticles within skin, from the stratum corneum to dermal layers. Mechanisms of drug penetration and penetration enhancer action have been elucidated.

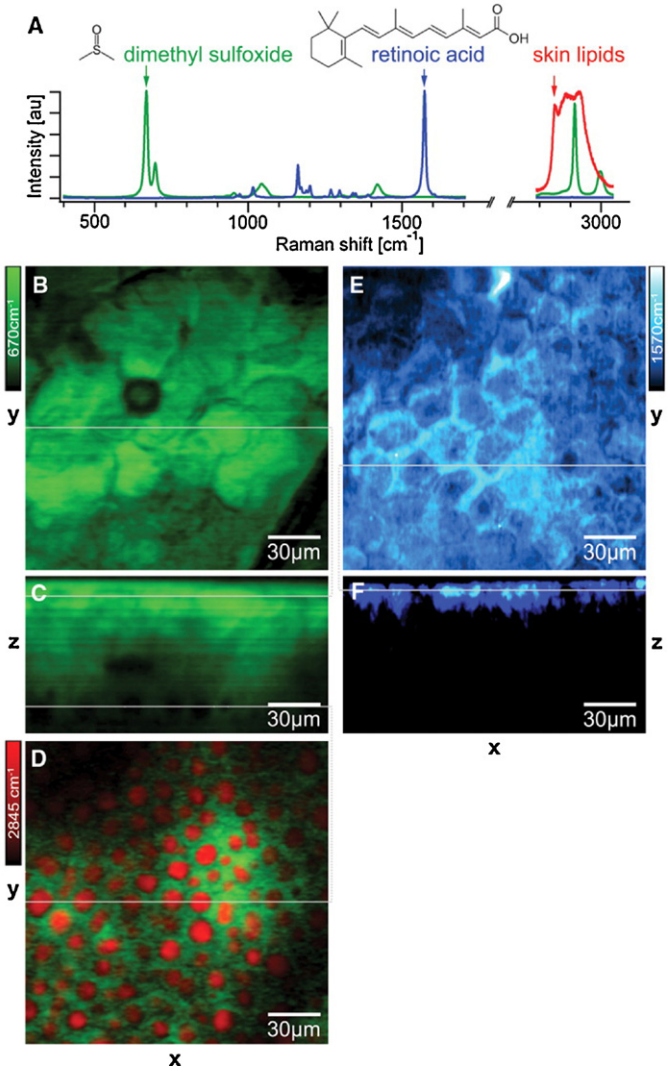

Fig. 6. Imaging drug penetration into mouse skin using SRS microscopy, (a) Raman spectra of dimethyl sulphoxide (DMSO, green), retinoic acid (blue), and lipids in mouse skin (red), (b) top view of the penetrated DMSO (green), (c) stimulated Raman loss (SRL) DMSO depth profile through the line in (b), (d) simultaneous SRL two colour image of DMSO (green) and lipid (red) at subcutaneous layer at a depth of about 65 μm though the lower line in (c), (e) top view of the penetrated retinoic acid (blue), and (f) retinoic acid depth profile through the line in (e). (For interpretation of the references to colour in this figure legend, the reader is referred to the web version of the article.)
Reproduced by the permission of the American Association for the Advancement of Science (Freudiger et al., 2008).

Such insights have not been possible using established dermal and transdermal delivery analysis methods, including the use of *in vitro* diffusion chambers and *in vivo* pharmacokinetics studies. The application of non-linear imaging to probe the fate within and across other tissue structures such as intestinal and ocular mucosa could also be useful.

3.3.2. Subcellular drug distribution

Non-linear imaging has allowed real-time analysis of subcellular distribution of drugs in live cells without labelling, and, as a result, mechanisms behind the action and inaction of drugs have been probed. Mouras et al. (2010) combined CARS, two-photon fluorescence, and SHG to image breast cancer tissue as well as drug delivery within live breast cancer cells. The autofluorescing elastin in the tissue was imaged from the two-photon fluorescence signals, while collagen generated the SHG signal. CARS signals were

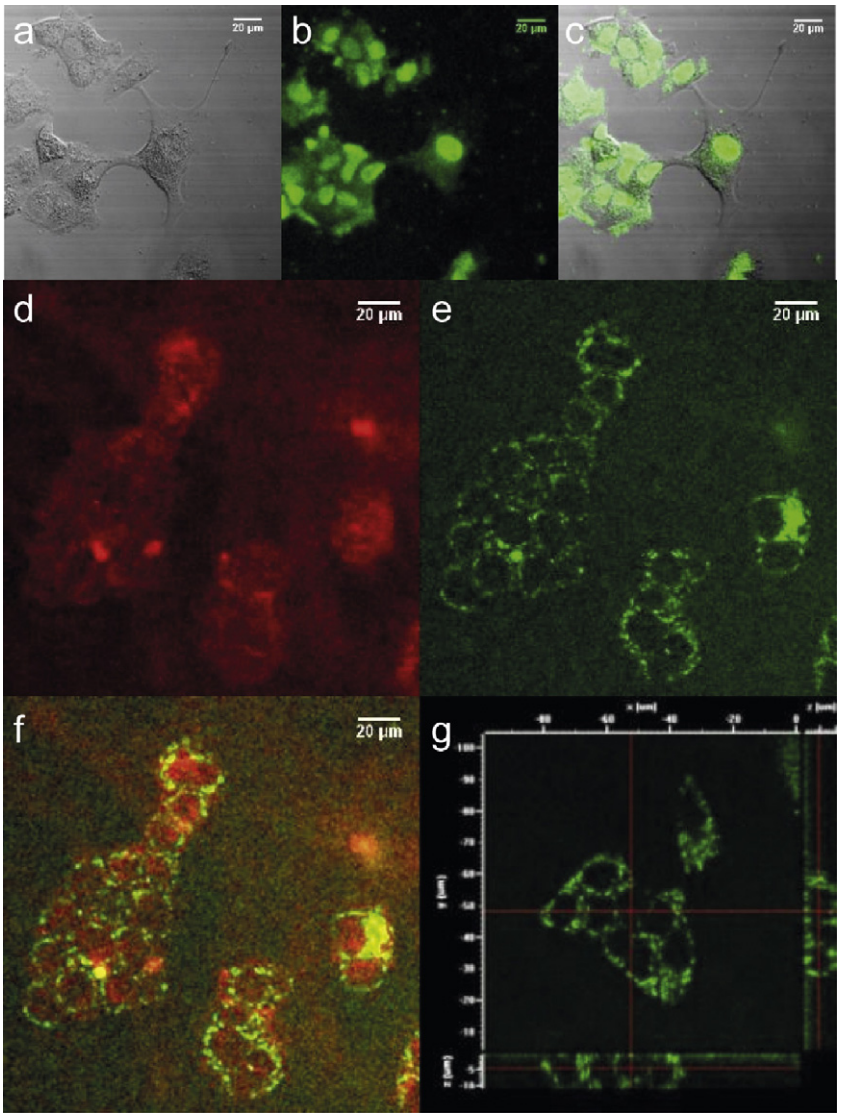

Fig. 7. Monitoring anticancer drugs in live carcinoma cells. Doxorubicin in MCF-7 WT cells: (a) transmission, (b) two-photon fluorescence of doxorubicin and (c) superposition of (a) and (b) showing the accumulation of doxorubicin molecules within the nuclei. Lipids and doxorubicin in MCF-7 DOX live cells: (d) CARS image at 2845 cm^{-1} corresponding to CH_2 in lipids highlighting the cytoplasm of the cells, (e) two-photon fluorescence image showing the distribution of doxorubicin, (f) superposition of (d) and (e) showing the preferential localisation of doxorubicin molecules at the perinuclear area and cytoplasm, and (g) 3D distribution of drug molecules within the cells (different cells from the same Petri dish). The drugs are completely surrounding the nuclei.
Reproduced by the permission of John Wiley & Sons, Inc. (Mouras et al., 2010).

generated from the protein (amide I band) and PO_2^- present in the DNA. The distribution of these signals within the tissue was used to identify tumour regions. Doxorubicin, a cytotoxic drug that exerts its cytotoxic effect by intercalating DNA, was incubated with human breast carcinoma cells (MCF-7). The drug was imaged using two-photon fluorescence because it is inherently fluorescent. The drug penetrated and concentrated into the nuclei of the wild-type (WT) cancer cells (Fig. 7). The drug was also incubated with doxorubicin resistant clones from the same cell line. Interestingly, in these cells there was fluorescent signal from the perinuclear area and cytoplasm of the cells, but not from within the nuclei themselves. This indicates that, in contrast to the susceptible cells, the drug concentration is negligible in the cell nuclei of the resistant cells. The high concentration in the perinuclear area supports the theory that there are high levels of P-glycoprotein in the plasma membranes that eject the drug from the nucleus and hence its site of action (Mouras et al., 2010). Two-photon fluorescence has also been used to image the distribution of toptican, another cytotoxic compound, in MCF-7 cells (Errington et al., 2005). In these cells, the drug localised in the nuclei and, to a lesser extent, the cytoplasm. The amount of intracellular (both cytoplasmic and nuclear) fluorescence varied between cells, with some cells demonstrating persistently low levels of fluorescence and, by implication, decreased susceptibility to the drug.

SRS has been used to monitor the uptake of omega-3 fatty acids by live human cancer lung cells (Freudiger et al., 2008). A band unique to unsaturated fatty acids at 3015 cm^{-1} was used to resolve eicosapaenoic acid from endogenous lipids, and its uptake and enrichment in the intracellular endogenous lipid domains was visualised. The authors suggest that the ability to image the uptake of unsaturated fatty acids into live cells could help with understanding lipid metabolism and associated diseases.

These studies demonstrate that label-free imaging of drug distribution within live target cells provides micropharmacokinetic profiles that can be used to determine whether the drug reaches its site of action within the cell, and heterogeneity within cell populations may be determined. Label-free imaging of non-fluorescing drugs remains a challenge due to limited sensitivity, but devel-

opments in sources (for optimised excitation), techniques (SRS, heterodyne) and intra-molecular labelling (where bonds with a high Raman activity are inserted rather than complete fluorescent labels) are progressing rapidly and the sensitivity is expected to improve considerably over the next five years. Intracellular drug imaging may help in the selection of drugs with appropriate cell and organelle penetrating properties early on in the drug discovery and development process.

3.3.3. Nanoparticle distribution within tissues and cells

The fate of nanoparticles used for drug delivery is of fundamental importance for drug targeting and safety. CARS microscopy has been used to investigate polymeric nanoparticle uptake by cells. In a study by Xu et al. (2009) poly(lactic-co-glycolic acid) (PLGA) nanoparticles were incubated with live carcinoma cells, and the particles were found not to be taken up by the cells in three hours. This contrasted with the prevailing belief based on the analyses of PLGA particles loaded with dyes and fluorescence markers resulting in fluorescence within cells. Since CARS microscopy directly probed the nanoparticles rather than any markers, it could be shown that the markers themselves rather than the particles were absorbed into the cells. The research also suggests that contact between drug loaded nanoparticles and the cell membrane facilitates drug uptake, at least in the case of small molecular weight and hydrophobic drugs, such as paclitaxel (Xu et al., 2009).

Scown et al. (2009) used CARS microscopy to investigate the fate of silver, titanium dioxide, zinc oxide and cerium (IV) oxide nanoparticles in trout liver cell cultures. Metal and metal oxide nanoparticles give rise to a resonant charge oscillation that greatly enhances the local field and therefore enhances the non-linear optical response (Wang et al., 2006), leading to large CARS signals that are independent of the vibrational signal being probed. This allows nanoparticles that are much smaller than the diffraction limit of the CARS system to be imaged. With the nanoparticles being much smaller than the spatial resolution of the microscope (about 200 nm), the degree of aggregation was indicated by the intensity of the signal. The CARS microscopy images suggested that the nanoparticles were internalised into the hepatocytes. Although this study was undertaken in an environmental toxicity context, it has relevance with respect to drug delivery involving metal and metal oxide nanoparticles.

Chen et al. (2009) used CARS microscopy to image engineered gold nanoparticles in mouse liver tissue. They found that the tissue accumulation was particle size dependent, with both *in vivo* toxicity and tissue accumulation of the nanoparticles occurring only for gold nanoparticles with diameters between 8 and 37 nm. Interestingly, larger particles did not result in acute toxicity, and, according to CARS microscopy, exhibited no or much less accumulation in the liver tissue (Chen et al., 2009).

As the prevalence of dosage forms utilising nanoparticles increases, non-linear imaging may play a vital role in better understanding the ability of nanoparticles to penetrate various tissues and cells during drug targeting, and the biological fate of the nanoparticles once their therapeutic purpose has been served.

4. Conclusion

The chemical, structural, spatial and temporal resolutions that can be obtained with non-linear imaging makes it well suited for the investigation of wide-ranging topics in pharmaceutics, with it having the potential to gain numerous insights that have been difficult or impossible to obtain with more established analysis methods. Analysis over the last few years has spanned the drug delivery spectrum, from probing relatively fundamental structural phenomena in drug delivery vehicles to imaging the subcellular distribution of drugs in cells. Despite this, research into pharmaceutical applications remains in its infancy, and many potential applications await its use. As the technology associated with non-linear imaging further develops and becomes more accessible, its use not only in academia, but also in the pharmaceutical industry will be watched with interest.

References

Boyd, R.W., 2008. Non-linear Optics, third edition. Academic Press, Burlington.

Carriles, R., Schafer, D.N., Sheetz, K.E., Field, J.J., Cisek, R., Barzda, V., Squier, J.A., 2009. Invited review article: Imaging techniques for harmonic and multiphoton absorption fluorescence microscopy. Rev. Sci. Instrum. 80, 081101 (invited review).

Carvell, M., Robb, I.D., Small, P.W., 1998. The influence of labelling mechanisms on the fluorescence behaviour of polymers bearing fluorescein labels. Polymer 39, 393–398.

Chen, Y.S., Hung, Y.C., Liau, I., Huang, G.S., 2009. Assessment of the *in vivo* toxicity of gold nanoparticles. Nanosc. Res. Lett. 4, 858–864.

Cheng, J.-X., 2007. Coherent anti-Stokes Raman scattering microscopy. Appl. Spectrosc. 61, 197–208.

Cheng, J.-X., Xie, X.S., 2004. Coherent anti-Stokes Raman scattering microscopy: instrumentation, theory, and applications. J. Phys. Chem. B 108, 827–840.

Chowdary, P.D., Benalcazar, W.A., Jiang, Z., Marks, D.M., Boppart, S.A., Gruebele, M., 2010. High speed non-linear interferometric vibrational analysis of lipids by spectral decomposition. Anal. Chem. 82, 3812–3818.

Clark, D., Henson, M., LaPlant, F., Šašić, S., Zhang, L., 2007. Pharmaceutical applications of mapping and imaging. In: Pivonka, D.E., Chalmers, J.M., Griffiths, P.R. (Eds.), Applications of Vibrational Spectroscopy in Pharmaceutical Research and Development. John Wiley & Sons, Ltd, pp. 309–335.

Day, J.P.R., Rago, G., Domke, K.F., Velikov, K.P., Bonn, M., 2010. Label-free imaging of lipophilic bioactive molecules during lipid digestion by multiplex coherent anti-Stokes Raman scattering microspectroscopy. J. Am. Chem. Soc. 132, 8433–8439.

Errington, R.J., Ameer-beg, S.M., Vojnovic, B., Patterson, L.H., Zloh, M., Smith, P.J., 2005. Advanced microscopy solutions for monitoring the kinetics and dynamics of drug-DNA targeting in living cells. Adv. Drug Deliv. Rev. 57, 153–167.

Evans, C.L., Potma, E.O., Puoris'haag, M., Cote, D., Lin, C.P., Xie, X.S., 2005. Chemical imaging of tissue *in vivo* with video-rate coherent anti-Stokes Raman scattering microscopy. Proc. Natl. Acad. Sci. U. S. A. 102, 16807–16812.

Evans, C.L., Potma, E.O., Xie, X.S., 2004. Coherent anti-Stokes Raman scattering spectral interferometry: determination of the real and imaginary components of non-linear susceptibility (3) for vibrational microscopy. Opt. Lett. 29, 2923–2925.

Evans, C.L., Xie, X.S., 2008. Coherent anti-Stokes Raman scattering microscopy: chemical imaging for biology and medicine. Annu. Rev. Anal. Chem. 1, 883–909.

Freudiger, C.W., Min, W., Saar, B.G., Lu, S., Holtom, G.R., He, C., Tsai, J.C., Kang, J.X., Xie, X.S., 2008. Label-free biomedical imaging with high sensitivity by Raman scattering microscopy. Science 322, 1857–1861.

Ganikhanov, F., Evans, C.L., Saar, B.G., Xie, X.S., 2006. High-sensitivity vibrational imaging with frequency modulation coherent anti-Stokes Raman scattering (FM CARS) microscopy. Opt. Lett. 31, 1872–1874.

Gendrin, C., Roggo, Y., Collet, C., 2008. Pharmaceutical applications of vibrational chemical imaging and chemometrics: a review. J. Pharm. Biomed. Anal. 48, 533–553.

Gordon, K.C., McGoverin, C.M., this issue. Raman mapping of pharmaceutics.

Groß, P., Kleinschmidt, L., Beer, S., Cleff, C., Fallnich, C., 2010. Single-laser light source for CARS microscopy based on soliton self-frequency shift in a microstructured fiber. Appl. Phys. B: Lasers Optics, 1–6.

Jurna, M., Garbacik, E.T., Korterik, J.P., Herek, J.L., Otto, C., Offerhaus, H.L., 2010. Visualizing resonances in the complex plane with vibrational phase contrast coherent anti-Stokes Raman scattering. Anal. Chem. 82, 7656–7659.

Jurna, M., Windbergs, M., Strachan, C.J., Hartsuiker, L., Otto, C., Kleinebudde, P., Herek, J.L., Offerhaus, H.L., 2009. Coherent anti-Stokes Raman scattering microscopy to monitor drug dissolution in different oral pharmaceutical tablets. J. Innovat. Optic. Health Sci. 2, 37–43.

Kang, E., Robinson, J., Park, K., Cheng, J.X., 2007. Paclitaxel distribution in poly(ethylene glycol)/poly(lactide-co-glycolic acid) blends and its release visualized by coherent anti-Stokes Raman scattering microscopy. J. Control. Release 122, 261–268.

Kang, E.N., Wang, H.F., Kwon, I.K., Robinson, J., Park, K., Cheng, J.X., 2006. In situ visualization of paclitaxel distribution and release by coherent anti-Stokes Raman scattering microscopy. Anal. Chem. 78, 8036–8043.

Kennedy, A.P., Sutcliffe, J., Cheng, J.X., 2005. Molecular composition and orientation in myelin figures characterized by coherent anti-Stokes Raman scattering microscopy. Langmuir 21, 6478–6486.

Kuo, T.-R., Wu, C.-L., Hsu, C.-T., Lo, W., Chiang, S.-J., Lin, S.-J., Dong, C.-Y., Chen, C.-C., 2009. Chemical enhancer induced changes in the mechanisms of transdermal delivery of zinc oxide nanoparticles. Biomaterials 30, 3002–3008.

Lee, J.-N., Jee, S.-H., Chan, C.-C., Lo, W., Dong, C.-Y., Lin, S.-J., 2008. The effects of depilatory agents as penetration enhancers on human stratum corneum structures. J. Invest. Dermatol. 128, 2240–2247.

Lin, S.J., Jee, S.H., Dong, C.Y., 2007. Multiphoton microscopy: a new paradigm in dermatological imaging. Eur. J. Dermatol. 17, 361–366.

Liu, Y., Lee, Y.J., Cicerone, M.T., 2009. Broadband CARS spectral phase retrieval using a time-domain Kramers–Kronig transform. Opt. Lett. 34, 1363–1365.
Mallick, B., Lakshmanna, A., Radhalakshmi, V., Umapathy, S., 2008. Design and development of stimulated Raman spectroscopy apparatus using a femtosecond laser system. Curr. Sci., 95.
McFearin, C.L., Beaman, D.K., Moore, F.G., Richmond, G.L., 2009. From Franklin to today: toward a molecular level understanding of bonding and adsorption at the oil–water interface. J. Phys. Chem. C 113, 1171–1188.
Mortensen, L.J., Oberdorster, G., Pentland, A.P., DeLouise, L.A., 2008. In vivo skin penetration of quantum dot nanoparticles in the murine model: the effect of UVR. Nano Lett. 8, 2779–2787.
Mouras, R., Rischitor, G., Downes, A., Salter, D., Elfick, A., 2010. Non-linear optical microscopy for drug delivery monitoring and cancer tissue imaging. J. Raman Spectrosc. doi:10.1002/jrs.2622.
Müller, M., Zumbusch, A., 2007. Coherent anti-Stokes Raman scattering microscopy. ChemPhysChem 8, 2157–2170.
Oheim, M., Michael, D.J., Geisbauer, M., Madsen, D., Chow, R.H., 2006. Principles of two-photon excitation fluorescence microscopy and other non-linear imaging approaches. Adv. Drug Deliv. Rev. 58, 788–808.
Oron, D., Dudovich, N., Silberberg, Y., 2002. Single-pulse phase-contrast non-linear Raman spectroscopy. Phys. Rev. Lett. 89, 273001.
Oudar, J.L., Smith, R.W., Shen, Y.R., 1979. Polarization-sensitive coherent anti-Stokes Raman spectroscopy. Appl. Phys. Lett. 34, 758–760.
Pautot, S., Frisken, B.J., Cheng, J.X., Xie, X.S., Weitz, D.A., 2003. Spontaneous formation of lipid structures at oil/water lipid interfaces. Langmuir 19, 10281–10287.
Ploetz, E., Marx, B., Klein, T., Huber, R., Gilch, P., 2009. A 75 MHz light source for femtosecond stimulated Raman microscopy. Opt. Express 17, 18612–18620.
Rinia, H.A., Bonn, M., Müller, M., Vartiainen, E.M., 2007. Quantitative CARS spectroscopy using the maximum entropy method: the main lipid phase transition. ChemPhysChem 8, 279–287.
Scown, T.M., Goodhead, R.M., Johnston, B.D., Moger, J., Baalousha, M., Lead, J.R., van Aerle, R., Iguchi, T., Tyler, C.R., 2009. Assessment of cultured fish hepatocytes for studying cellular uptake and (eco)toxicity of nanoparticles. Environ. Chem. 7, 36–49.
Slipchenko, M.N., Chen, H., Ely, D.R., Jung, Y., Carvajal, M.T., Cheng, J.-X., 2010. Vibrational imaging of tablets by epi-detected stimulated Raman scattering microscopy. Analyst. doi:10.1039/C0AN00252F.
Stracke, F., Weiss, B., Lehr, C.-M., Konig, K., Schaefer, U.F., Schneider, M., 2006. Multiphoton microscopy for the investigation of dermal penetration of nanoparticle-borne drugs. J. Invest. Dermatol. 126, 2224–2233.
Sun, Y., Lo, W., Lin, S.J., Jee, S.H., Dong, C.Y., 2004. Multiphoton polarization and generalized polarization microscopy reveal oleic-acid-induced structural changes in intercellular lipid layers of the skin. Opt. Lett. 29, 2013–2015.
Tsung-Hua, T., Shiou-Hwa, J., Chen-Yuan, D., Sung-Jan, L., 2009. Multiphoton microscopy in dermatological imaging. J. Dermatol. Sci. 56, 1–8.
van Rhijn, A.C.W., Offerhaus, H.L., van der Walle, P., Herek, J.L., Jafarpour, A., 2010. Exploring, tailoring, and traversing the solution landscape of a phase-shaped CARS process. Opt. Express 18, 2695–2709.
Volkmer, A., Book, L.D., Xie, X.S., 2002. Time-resolved coherent anti-Stokes Raman scattering microscopy: imaging based on Raman free induction decay. Appl. Phys. Lett. 80, 1505–1507.
von Vacano, B., Motzkus, M., 2006. Time-resolved two color single-beam CARS employing supercontinuum and femtosecond pulse shaping. Opt. Commun. 264, 488–493.
Wang, H., Brandl, D.W., Nordlander, P., Halas, N.J., 2006. Plasmonic nanostructures: artificial molecules. Acc. Chem. Res. 40, 53–62.
Windbergs, M., Jurna, M., Offerhaus, H.L., Herek, J.L., Kleinebudde, P., Strachan, C.J., 2009. Chemical imaging of oral solid dosage forms and changes upon dissolution using coherent anti-Stokes Raman scattering microscopy. Anal. Chem. 81, 2085–2091.
Xu, P.S., Gullotti, E., Tong, L., Highley, C.B., Errabelli, D.R., Hasan, T., Cheng, J.X., Kohane, D.S., Yeo, Y., 2009. Intracellular drug delivery by poly(lactic-co-glycolic acid) nanoparticles, revisited. Mol. Pharm. 6, 190–201.
Yu, B., Dong, C.Y., So, P.T., Blankschtein, D., Langer, R., 2001. In vitro visualization and quantification of oleic acid induced changes in transdermal transport using two-photon fluorescence microscopy. J. Invest. Dermatol. 117, 16–25.
Yu, B., Kim, K.H., So, P.T., Blankschtein, D., Langer, R., 2003. Visualization of oleic acid-induced transdermal diffusion pathways using two-photon fluorescence microscopy. J. Invest. Dermatol. 120, 448–455.
Yuratich, M.A., Hanna, D.C., 1977. Coherent anti-Stokes Raman spectroscopy (CARS)—selection rules, depolarization ratios and rotational structure. Mol. Phys. 33, 671–682.